

# Learning to Track at 100 FPS with Deep Regression Networks

David Held, Sebastian Thrun, and Silvio Savarese

Computer Science Department, Stanford University  
{davheld, thrun, ssilvio}@cs.stanford.edu

**Abstract.** Machine learning techniques are often used in computer vision due to their ability to leverage large amounts of training data to improve performance. Unfortunately, most generic object trackers are still trained from scratch online and do not benefit from the large number of videos that are readily available for offline training. We propose a method for using neural networks to track generic objects in a way that allows them to improve performance by training on labeled videos. Previous attempts to use neural networks for tracking are very slow to run and not practical for real-time applications. In contrast, our tracker uses a simple feed-forward network with no online training required, allowing our tracker to run at 100 fps during test time. Our tracker trains from both labeled video as well as a large collection of images, which helps prevent overfitting. The tracker learns generic object motion and can be used to track novel objects that do not appear in the training set. We test our network on a standard tracking benchmark to demonstrate our tracker’s state-of-the-art performance. Our network learns to track generic objects in real-time as they move throughout the world.

**Keywords:** Tracking, deep learning, neural networks, machine learning

## 1 Introduction

Given some object of interest marked in one frame of a video, the goal of “single-target tracking” is to locate this object in subsequent video frames, despite object motion, changes in viewpoint, lighting changes, or other variations. Single-target tracking is an important component of many systems. For person-following applications, a robot must track a person as they move through their environment. For autonomous driving, a robot must track dynamic obstacles in order to estimate where they are moving and predict how they will move in the future.

Generic object trackers (trackers that are not specialized for specific classes of objects) are traditionally trained entirely from scratch online (i.e. during test time) [1,2,3,4], with no offline training being performed. Such trackers suffer in performance because their only knowledge of the world is from their online training. Trackers that are only trained online cannot take advantage of the large number of videos that are readily available that can be used to improve their performance. Such offline training videos can be used to teach the tracker

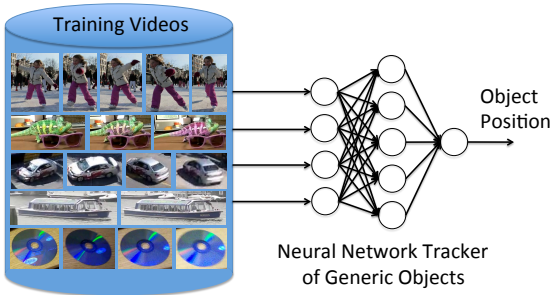


**Fig. 1.** Using a collection of videos and images with bounding box labels (but no class information), we train a neural network to track generic objects. Our network observes how objects move and outputs the resulting object motion, which is used for tracking.

to handle rotations, changes in viewpoint, lighting changes, or other complex challenges.

In many other areas of computer vision, machine learning has allowed vision algorithms to train from lots of offline data and learn about the world [5]. For example, neural networks have been trained for image classification [6], object detection [7], age and gender classification [8], and activity recognition [9]. In each of these cases, the network is trained offline from many examples, and its performance improves as it iterates through the training set of images. Such models benefit from the ability of neural networks to learn complex functions from large amounts of data.

In this work, we ask if it is possible to learn to track generic objects in real-time by watching videos offline of objects moving in the world. To achieve this goal, we introduce *GOTURN*, Generic Object Tracking Using Regression Networks. We train a neural network for tracking in an entirely offline manner with training videos and images (shown in Figure 1). The tracker learns how to track generic objects; given a test sequence of frames for a novel object, the network will regress to the location of the target object in each frame. Because our training is done entirely offline, at test time our tracker requires just a single feed-forward pass through the network, tracking objects at 100 fps (although the videos were recorded at a lower frame rate). Through the offline training procedure, the tracker learns to track novel objects in a fast, robust, and accurate manner.

To train the tracker offline, we require a training set of videos that are labeled with the location of some object in each frame of the video. Our tracker can also leverage a large training set of labeled images, which allows our tracker to learn to track a variety of object types and prevents overfitting. Our tracker does not require any class-level labeling or information about the types of objects being tracked.

Although some initial work has been done in using neural networks for tracking, these efforts have produced neural-network trackers that are trained online

and thus are too slow for practical use [10,11,12,13,14,15,16,17,18]. Because our tracker is trained offline to learn a generic relationship between appearance and motion, no online training of our tracker is required. At test time, our tracker requires just a single feed-forward pass through the network and directly regresses to the location of the tracked object, allowing us to track objects at 100 fps.

GOTURN is the first generic object tracker that is trained entirely offline. We use a standard tracking benchmark to demonstrate that our tracker outperforms state-of-the-art trackers. By watching many videos of moving objects, our tracker learns the relationship between appearance and motion that allows it to track new objects at test time. GOTURN establishes a new framework for tracking in which the relationship between appearance and motion is learned offline in a generic manner.

## 2 Related Work

**Online training for tracking.** Trackers for generic object tracking are typically trained entirely online, starting from the first frame of a video [1,2,3,4]. A typical tracker will sample patches near the target object, which are considered as “foreground” [2]. Some patches farther from the target object are also sampled, and these are considered as “background.” These patches are then used to train a foreground-background classifier, and this classifier is used to score patches from the next frame to estimate the new location of the target object [3]. Such a classifier can also be combined with optical flow estimates [4]. Unfortunately, since these trackers are trained entirely online, they cannot take advantage of the large amount of videos that are readily available for offline training that can potentially be used to improve their performance.

Some researchers have also attempted to use neural networks for tracking within the traditional online training framework [10,11,12,13,14,15,16,17,18,19], showing state-of-the-art results [15,17,20]. Unfortunately, neural networks are very slow to train, and if online training is required, then the resulting tracker will be very slow at test time. Such trackers range from 0.8 fps [10] to 15 fps [13], with the top performing neural-network trackers running at 1 fps on a GPU [15,17,20]. Hence, these trackers are not usable for most practical applications. Because our tracker is trained offline from many training videos, no online training of our tracker is required. At test time, our tracker requires just a single feed-forward pass through the network and directly regresses to the location of the tracked object, enabling us to track objects at 100 fps.

**Model-based trackers.** A separate class of trackers are the model-based trackers which are designed to track a specific class of objects [21,22,23]. For example, if one is only interested in tracking pedestrians, then one can train a pedestrian detector. During test-time, these detections can be linked together using temporal information. These trackers are trained offline, but they are limited because they can only track a specific class of objects. Our tracker is trained offline in a generic fashion and can be used to track novel objects at test time.

**Other neural network tracking frameworks.** Others have attempted to use neural networks for tracking in various ways, such as metric learning [24] or visual attention models [25,26]. However, these approaches exhibit poor performance when evaluated on difficult tracker datasets, and they are not competitive with other state-of-the-art trackers.

### 3 Method

#### 3.1 Method Overview

At a high level, we feed frames of a video into a neural network, and the network successively outputs the location of the tracked object in each frame. We train the tracker entirely offline with video sequences and images. Through our offline training procedure, our tracker learns a generic relationship between appearance and motion that can be used to track novel objects at test time with no online training required.

#### 3.2 Input / output format

**What to track.** In case there are multiple objects in the video, the network must receive some information about which object in the video is being tracked. To achieve this, we input an image of the target object into the network. We crop and scale the previous frame to be centered on the target object, as shown in Figure 2. If there are multiple objects in the video, the network learns to track the object that is located at the center of this crop. We pad this crop to allow the network to receive some contextual information about the surroundings of the target object. This input allows our network to track novel objects that it has not seen before; the network will track whatever object is being input in this crop.

In more detail, suppose that in frame  $t - 1$ , our tracker previously predicted that the target was located in a bounding box centered at  $c = (c_x, c_y)$  with a width of  $w$  and a height of  $h$ . At time  $t$ , we take a crop of frame  $t - 1$  centered at  $(c_x, c_y)$  with a width and height of  $k_1 w$  and  $k_1 h$ , respectively. This crop tells the network which object is being tracked. The value of  $k_1$  determines how much context the network will receive about the target object from the previous frame.

**Where to look.** To find the target object in the current frame, the tracker should know where the object was previously located. Since objects tend to move smoothly through space, the previous location of the object will provide a good guess of where the network should expect to currently find the object. We achieve this by choosing a search region in our current frame based on the object’s previous location. We crop the current frame using the search region and input this crop into our network, as shown in Figure 2. The goal of the network is then to regress to the location of the target object within the search region.

In more detail, the crop of the current frame  $t$  is centered at  $c' = (c'_x, c'_y)$ , where  $c'$  is the expected mean location of the target object. We set  $c' = c$ , which

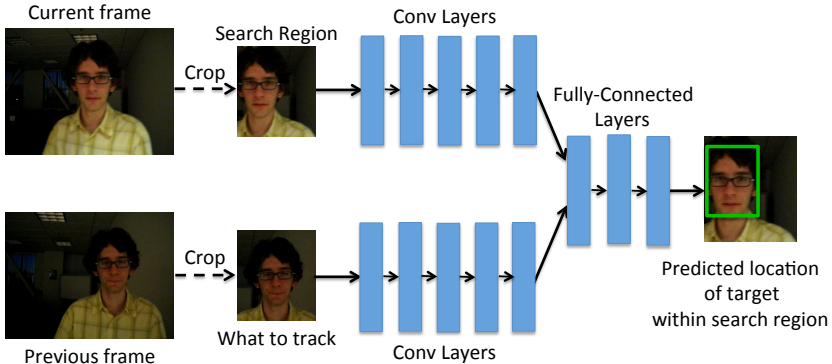


**Fig. 2.** Our network architecture for tracking. We input to the network a search region from the current frame and a target from the previous frame. The network learns to compare these crops to find the target object in the current image.

is equivalent to a constant position motion model, although more sophisticated motion models can be used as well. The crop of the current frame has a width and height of  $k_2 w$  and  $k_2 h$ , respectively, where  $w$  and  $h$  are the width and height of the predicted bounding box in the previous frame, and  $k_2$  defines our search radius for the target object. In practice, we use  $k_1 = k_2 = 2$ .

As long as the target object is not moving too quickly, the target will be located within this region. For fast-moving objects, the size of the search region could be increased, at a cost of increasing the complexity of the network. Alternatively, to handle large movements, our tracker can be combined with another approach such as an online-trained object detector, as in the TLD framework [4], or a visual attention model [25,26,27]; we leave this for future work.

**Network output.** The network outputs the coordinates of the object in the current frame, relative to the search region. The network’s output consists of the coordinates of the top left and bottom right corners of the bounding box.

### 3.3 Network architecture

For single-target tracking, we define a novel image-comparison architecture, shown in Figure 2. In this model, we input the target object as well as the search region each into a sequence of convolutional layers. The output of these convolutional layers is a set of features that capture a high-level representation of the image.

The outputs of these convolutional layers are then fed through a number of fully connected layers. The role of the fully connected layers is to compare the features from the target object to the features in the current frame to find where the target object has moved. In some cases, the object may have undergone a simple translation; in other cases, there can be rotations, lighting changes, occlusions, or deformations. The function learned by the fully connected layers

is thus a complex feature comparison which is learned through many examples to be robust to these various factors while outputting the relative motion of the tracked object.

In more detail, the convolutional layers in our model are taken from the first five convolutional layers of the CaffeNet architecture [28] (a minor variation of AlexNet [6]). We take the output of these convolutional layers (i.e. the pool5 features [28]) from the crops from the previous frame and the current frame, and we flatten each of these features into a vector. We then concatenate these vectors into a single vector. This vector is input to 3 fully connected layers, each with 4096 nodes. Finally, we connect the last fully connected layer to an output layer that contains 4 nodes which represent the output bounding box. We scale the output by a factor of 10, chosen using our validation set (as with all of our hyperparameters). Network hyperparameters are taken from the defaults for CaffeNet, and between each layer we use dropout, ReLU, and maxpool nonlinearities as in CaffeNet. Our neural network is implemented using Caffe [28]. We will perform experiments that will help us to understand how this network is able to robustly track objects.

### 3.4 Tracking

During test time, we initialize the tracker with a ground-truth bounding box from the first frame, denoting the location of the target object, as is standard practice for single-target tracking. We crop the first and second frames as described in Section 3.2, and we feed the crops into the network to predict where the object has moved in the second frame. We continue in this manner, inputting crops from frame  $t - 1$  and frame  $t$  into the network to predict where the object is located in frame  $t$ . We continue to re-crop and feed pairs of frames into our network for the remainder of the video, and our network will track the movement of the target object throughout the entire video sequence.

## 4 Training

We train our network with a combination of videos and still images. The training procedure is described below. In both cases, we train the network with an L1 loss between the predicted bounding box and the ground-truth bounding box.

### 4.1 Training from Videos and Images

Our training set consists of a collection of videos in which a subset of frames in each video are labeled with the location of some object. For each successive pair of frames in the training set, we crop the frames as described in Section 3.2. During training time, we feed this pair of frames into the network and attempt to predict how the object has moved from the first frame to the second frame (shown in Figure 3). We also augment these training examples, as described in Section 4.2.

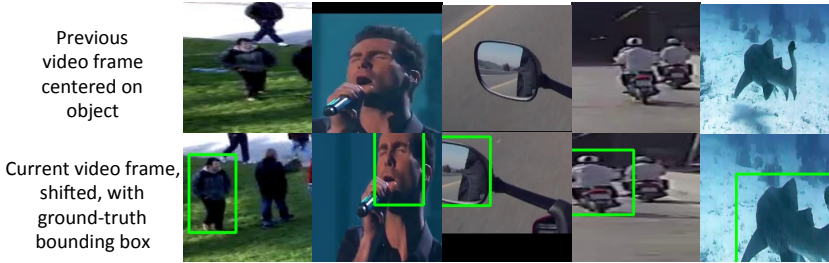


**Fig. 3.** Examples of training videos. The goal of the network is to predict the location of the target object shown in the center of the image in the top row, after being shifted as in the bottom row. The ground-truth bounding box is marked in green.

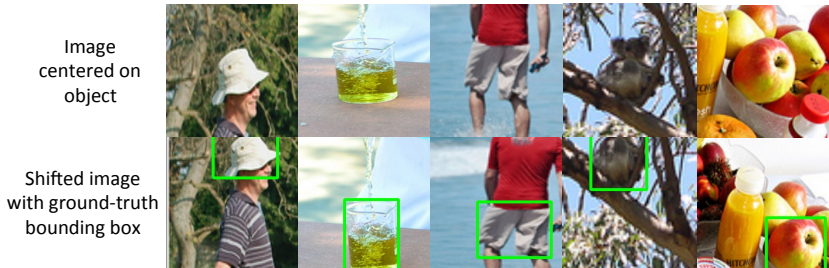


**Fig. 4.** Examples of training images. The goal of the network is to predict the location of the target object shown in the center of the image crop in the top row, after being shifted as in the bottom row. The ground-truth bounding box is marked in green.

Our training procedure can also take advantage of a set of still images that are each labeled with the location of an object. This training set of images teaches our network to track a more diverse set of objects and prevents overfitting to the objects in our training videos. To train our tracker from an image, we take random crops of the image, as shown in Figure 4. Between these two crops, the target object has undergone an apparent translation and scale change (see Figure 4). We treat these crops as if they were taken from different frames of a video. Although the “motions” in these crops are less varied than the types of motions found in our training videos, these images are still useful to train our network to track a variety of different objects.

## 4.2 Learning Motion Smoothness

Objects in the real-world tend to move smoothly through space. Given an ambiguous image in which the location of the target object is uncertain, a tracker should predict that the target object is located near to the location where it was previously observed. This is especially important in videos that contain multiple

nearly-identical objects, such as multiple fruit of the same type. Thus we wish to teach our network that, all else being equal, small motions are preferred to large motions.

To concretize the idea of motion smoothness, we model the center of the bounding box in the current frame  $(c'_x, c'_y)$  relative to the center of the bounding box in the previous frame  $(c_x, c_y)$  as

$$c'_x = c_x + w \cdot \Delta x \quad (1)$$

$$c'_y = c_y + h \cdot \Delta y \quad (2)$$

where  $w$  and  $h$  are the width and height, respectively, of the bounding box of the previous frame. The terms  $\Delta x$  and  $\Delta y$  are random variables that capture the change in position of the bounding box relative to its size. In our training set, we find that objects change their position such that  $\Delta x$  and  $\Delta y$  can each be modeled with a Laplace distribution with a mean of 0 (see Appendix F for details). Such a distribution places a higher probability on smaller motions than larger motions.

Similarly, we model size changes by

$$w' = w \cdot \gamma_w \quad (3)$$

$$h' = h \cdot \gamma_h \quad (4)$$

where  $w'$  and  $h'$  are the current width and height of the bounding box and  $w$  and  $h$  are the previous width and height of the bounding box. The terms  $\gamma_w$  and  $\gamma_h$  are random variables that capture the size change of the bounding box. We find in our training set that  $\gamma_w$  and  $\gamma_h$  are modeled by a Laplace distribution with a mean of 1. Such a distribution gives a higher probability on keeping the bounding box size near the same as the size from the previous frame.

To teach our network to prefer small motions to large motions, we augment our training set with random crops, where the random crops are drawn from the Laplace distributions described above. See Figures 3 and 4 for examples of such crops. Because these training examples are sampled from a Laplace distribution, small motions will be sampled more frequently than large motions, and thus our network will learn to prefer small motions to large motions. Note that this distribution does not place any hard constraints on our tracker; it simply makes our network more likely to predict small motions rather than large ones, all else being equal. We will show that this Laplace cropping procedure improves the performance of our tracker compared to the standard uniform cropping procedure used in classification tasks [6].

The scale parameters for the Laplace distributions are chosen via cross-validation to be  $b_x = 1/5$  (for the motion of the bounding box center) and  $b_s = 1/15$  (for the change in bounding box size). We constrain the random crop such that it must contain at least half of the target object in each dimension. We also limit the size changes such that  $\gamma_w, \gamma_h \in (0.6, 1.4)$ , to avoid overly stretching or shrinking the bounding box in a way that would be difficult for the network to learn.



### 4.3 Training procedure

To train our network, each training example is alternately taken from a video or from an image. When we use a video training example, we randomly choose a video, and we randomly choose a pair of successive frames in this video. We then take  $k_3$  random crops of the current frame, using the cropping procedure described in Section 4.2. Next, we randomly sample an image, and we take  $k_4$  random crops of this image, again using the procedure described in Section 4.2. We continue sampling images and video frames until our batch is full, and we then use this batch to train our network. In our experiments, we use  $k_3 = k_4 = 10$ , and we use a batch size of 50.

The convolutional layers in our network are pre-trained on ImageNet [29,30]. Because of our limited training set size, we do not fine-tune these layers to prevent overfitting. We train this network with a learning rate of 1e-5, and other hyperparameters are taken from the defaults for CaffeNet [28].

## 5 Experimental Setup

### 5.1 Training set

As described in Section 4, we train our network using a combination of videos and still images. Our training videos come from ALOV300++ [31], a collection of 314 video sequences. We remove 7 of these videos that overlap with our test set (see Appendix G for details), leaving us with 307 videos to be used for training. In this dataset, approximately every 5th frame of each video has been labeled with the location of some object being tracked. These videos are generally short, ranging from a few seconds to a few minutes in length. We split these videos into 251 for training and 56 for validation / hyper-parameter tuning. The training set consists of a total of 13,082 images of 251 different objects, or an average of 52 frames per object. The validation set consists of 2,795 images of 56 different objects. After choosing our hyperparameters, we retrain our model using our entire training set (training + validation). After removing the 7 overlapping videos, there is no overlap between the videos in the training and test sets.

Our training procedure also leveraged a set of still images that were used for training, as described in Section 4.1. These images were taken from the training set of the ImageNet Detection Challenge [29], in which 478,807 objects were labeled with bounding boxes. We randomly crop these images during training time, as described in Section 4.2, to create an apparent translation or scale change between two random crops. The random cropping procedure is only useful if the labeled object does not fill the entire image; thus, we filter those images for which the bounding box fills at least 66% of the size of the image in either dimension (chosen using our validation set). This leaves us with a total of 239,283 annotations from 134,821 images. These images help prevent overfitting by teaching our network to track objects that do not appear in the training videos.

## 5.2 Test set

Our test set consists of the 25 videos from the VOT 2014 Tracking Challenge [32]. We could not test our method on the VOT 2015 challenge [20] because there would be too much overlap between the test set and our training set. However, we expect the general trends of our method to still hold.

The VOT 2014 Tracking Challenge [32] is a standard tracking benchmark that allows us to compare our tracker to a wide variety of state-of-the-art trackers. The trackers are evaluated using two standard tracking metrics: accuracy ( $A$ ) and robustness ( $R$ ) [32,33], which range from 0 to 1. We also compute accuracy errors ( $1 - A$ ), robustness errors ( $1 - R$ ), and overall errors  $1 - (A + R)/2$ .

Each frame of the video is annotated with a number of attributes: occlusion, illumination change, motion change, size change, and camera motion. The trackers are also ranked in accuracy and robustness separately for each attribute, and the rankings are then averaged across attributes to get a final average accuracy and robustness ranking for each tracker. The accuracy and robustness rankings are averaged to get an overall average ranking.

## 6 Results

### 6.1 Overall performance

The performance of our tracker is shown in Figure 5, and further details can be found in Appendix H. Figure 5 demonstrates that our tracker has good robustness and performs near the top in accuracy. Further, our overall ranking (computed as the average of accuracy and robustness) outperforms all previous trackers on this benchmark. We have thus demonstrated the value of offline training for improving tracking performance. Moreover, these results were obtained after training on only 307 short videos. Further analysis in Appendix A suggests that large gains could be achieved if the training set size were increased by labeling more videos.

On an nVidia GTX 680 GPU, our tracker runs at an average of 9.98 ms per frame, or 100 fps (although the videos were recorded at a lower frame rate). If only a CPU is available, the tracker runs at 2.7 fps. Because our tracker is able to perform all of its training offline, during test time the tracker requires only a single feed-forward pass through the network, and thus the tracker is able to run at real-time speeds.

We compare the speed and rank of our tracker compared to the 38 other trackers submitted to the VOT 2014 Tracking Challenge [32] in Figure 6, using the overall rank score described in Section 5.2. We show the runtime of the tracker in EFO units (Equivalent Filter Operations), which normalizes for the type of hardware that the tracker was tested on [32]. Figure 6 demonstrates that ours was one of the fastest trackers compared to the 38 other baselines, while outperforming all other methods in the overall rank (computed as the average of the accuracy and robustness ranks). Note that some of these other trackers, such as ThunderStruck [32], also use a GPU.

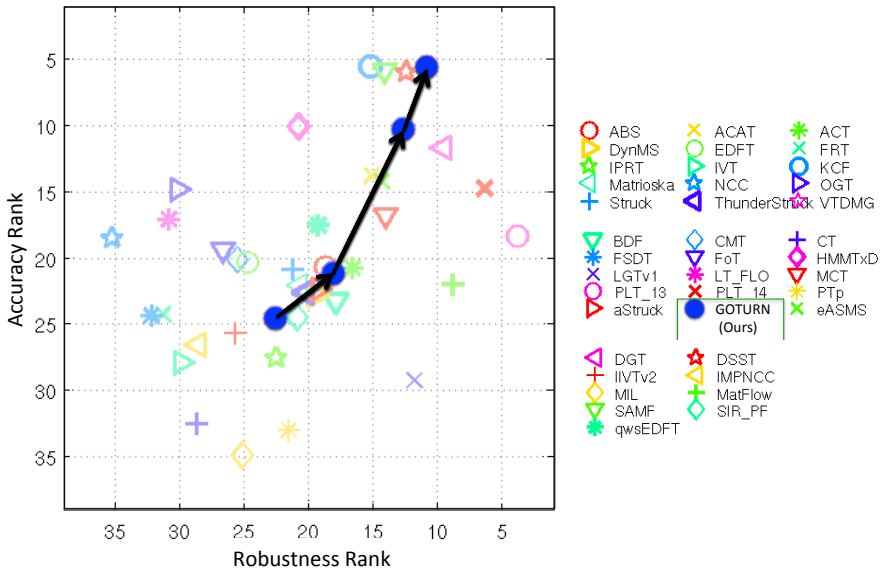


**Fig. 5.** Tracking results from the VOT 2014 tracking challenge. Our tracker’s performance is indicated with a blue circle, outperforming all previous methods on the overall rank (average of accuracy and robustness ranks). Our tracker has good robustness (x-axis) and near the top accuracy (y-axis). Our performance improves as we add more training videos, as shown by the black line.

Our tracker is able to track objects in real-time due to two aspects of our model: First, we learn a generic tracking model offline, so no online training is required. Online training of neural networks tends to be very slow, preventing real-time performance. Online-trained neural network trackers range from 0.8 fps [10] to 15 fps [13], with the top performing trackers running at 1 fps on a GPU [15,17,20]. Second, most trackers evaluate a finite number of samples and choose the highest scoring one as the tracking output. With a sampling approach, the accuracy is limited by the number of samples, but increasing the number of samples also increases the computational complexity. On the other hand, our tracker regresses directly to the output bounding box, so GOTURN achieves accurate tracking with no extra computational cost, running at 100 fps.

## 6.2 How does it work?

How does our neural-network tracker work? There are two hypotheses that one might propose:

1. The network compares the previous frame to the current frame to find the target object in the current frame.
2. The network acts as a local generic “object detector” and simply locates the nearest “object.”

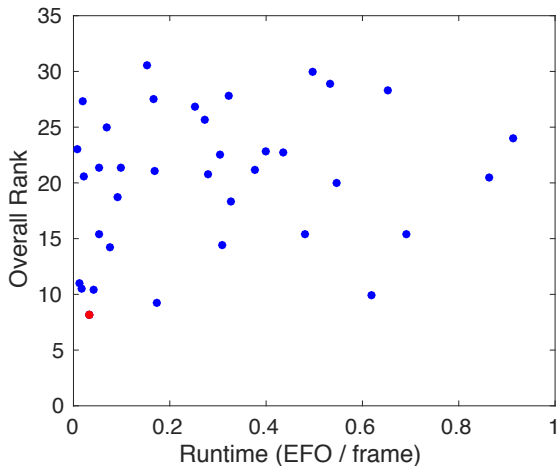


**Fig. 6.** Rank vs runtime of our tracker (red) compared to the 38 baseline methods from the VOT 2014 Tracking Challenge (blue). Each blue dot represents the performance of a separate baseline method (best viewed in color). Accuracy and robustness metrics are shown in Appendix D.

We differentiate between these hypotheses by comparing the performance of our network (shown in Figure 2) to the performance of a network which does not receive the previous frame as input (i.e. the network only receives the current frame as input). For this experiment, we train each of these networks separately. If the network does not receive the previous frame as input, then the tracker can only act as a local generic object detector (hypothesis 2).

Figure 7 shows the degree to which each of the hypotheses holds true for different tracking conditions. For example, when there is an occlusion or a large camera motion, the tracker benefits greatly from using the previous frame, which enables the tracker to “remember” which object is being tracked. Figure 7 shows that the tracker performs much worse in these cases when the previous frame is not included. In such cases, hypothesis 1 plays a large role, i.e. the tracker is comparing the previous frame to the current frame to find the target object.

On the other hand, when there is a size change or no variation, the tracker performs slightly worse when using the previous frame (or approximately the same). Under a large size change, the corresponding appearance change is too drastic for our network to perform an accurate comparison between the previous frame and the current frame. Thus the tracker is acting as a local generic object detector in such a case and hypothesis 2 is dominant. Each hypothesis holds true in varying degrees for different tracking conditions, as shown in Figure 7.

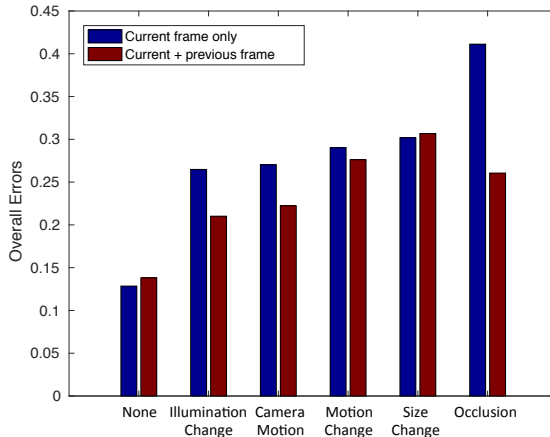


**Fig. 7.** Overall tracking errors for our network which receives as input both the current and previous frame, compared to a network which receives as input only the current frame (lower is better). This comparison allows us to disambiguate between two hypotheses that can explain how our neural-network tracker works (see Section 6.2). Accuracy and robustness metrics are shown in Appendix E.

### 6.3 Generality vs Specificity

How well can our tracker generalize to novel objects not found in our training set? For this analysis, we separate our test set into objects for which at least 25 videos of the same class appear in our training set and objects for which fewer than 25 videos of that class appear in our training set. Figure 8 shows that, even for test objects that do not have any (or very few) similar objects in our training set, our tracker performs well. The performance continues to improve even as videos of unrelated objects are added to our training set, since our tracker is able to learn a generic relationship between an object’s appearance change and its motion that can generalize to novel objects.

Additionally, our tracker can also be specialized to track certain objects particularly well. Figure 8 shows that, for test objects for which at least 25 videos of the same class appear in the training set, we obtain a large improvement as more training videos of those types of objects are added. This allows the user to specialize the tracker for particular applications. For example, if the tracker is being used for autonomous driving, then the user can add more objects of people, bikes, and cars into the training set, and the tracker will learn to track those objects particularly well. At the same time, Figure 8 also demonstrates that our tracker can track novel objects that do not appear in our training set, which is important when tracking objects in uncontrolled environments.

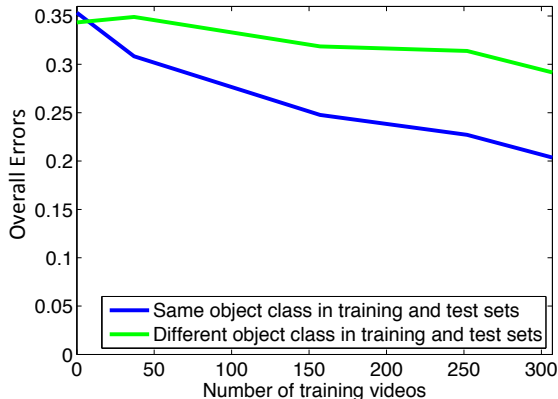


**Fig. 8.** Overall tracking errors for different types of objects in our test set as a function of the number of videos in our training set (lower is better). Class labels are not used by our tracker; these labels were obtained only for the purpose of this analysis. Accuracy and robustness metrics are shown in Appendix C.

## 6.4 Ablative Analysis

In Table 1, we show which components of our system contribute the most to our performance. We train our network with random cropping from a Laplace distribution to teach our tracker to prefer small motions to large motions (e.g. motion smoothness), as explained in Section 4.2. Table 1 shows the benefit of this approach compared to the baseline of uniformly sampling random crops (“No motion smoothness”), as is typically done for classification [6]. As shown, we reduce errors by 20% by drawing our random crops from a Laplace distribution.

Table 1 also shows the benefit of using an L1 loss compared to an L2 loss. Using an L1 loss significantly reduces the overall tracking errors from 0.43 to 0.24. Because the L2 penalty is relatively flat near 0, the network does not sufficiently penalize outputs that are close but not correct, and the network would often output a bounding box that was slightly too large or too small. When applied to a sequence of frames, the bounding box would grow or shrink without bound until the predicted bounding box was just a single point or the entire image. In contrast, an L1 loss penalizes more harshly answers that are only slightly incorrect, which keeps the bounding box size closer to the correct size and prevents the bounding box from shrinking or growing without bound.

We train our tracker using a combination of images and videos. Table 1 shows that, given the choice between images and videos, training on only videos gives a much bigger improvement to our tracker performance. At the same time, training on both videos and images gives the maximum performance for our tracker. Training on a small number of labeled videos has taught our tracker to be invariant to background motion, out-of-plane rotations, deformations, lighting changes, and occlusions. Training from a large number of labeled images has

GOTURN Variant	Overall errors	Accuracy errors	Robustness errors
L2 loss	0.43	0.69	0.17
No motion smoothness	0.30	0.48	0.13
Image training only	0.35	0.54	0.16
Video training only	0.29	0.44	0.13
<b>Full method (Ours)</b>	<b>0.24</b>	<b>0.39</b>	<b>0.10</b>

**Table 1.** Comparing our full GOTURN tracking method to various modified versions of our method to analyze the effect of different components of the system.

taught our network how to track a wide variety of different types of objects. By training on both videos and images, our tracker learns to track a variety of object types under different conditions, achieving maximum performance.

## 7 Conclusions

We have demonstrated how we can train a generic object tracker offline such that its performance improves by watching more training videos. During test time, we run the network in a purely feed-forward manner with no online fine-tuning required, allowing the tracker to run at 100 fps. Our tracker learns a generic relationship between an object’s appearance and its motion, allowing our tracker to track novel objects at test time to achieve state-of-the-art tracking performance. Our tracker thus demonstrates a new framework for tracking in which we can train a tracker offline to learn generic properties about object motion and appearance.

## References

1. Hare, S., Saffari, A., Torr, P.H.: Struck: Structured output tracking with kernels. In: Computer Vision (ICCV), 2011 IEEE International Conference on, IEEE (2011) 263–270
2. Babenko, B., Yang, M.H., Belongie, S.: Visual tracking with online multiple instance learning. In: Computer Vision and Pattern Recognition, 2009. CVPR 2009. IEEE Conference on, IEEE (2009) 983–990
3. Wang, N., Shi, J., Yeung, D.Y., Jia, J.: Understanding and diagnosing visual tracking systems. arXiv preprint arXiv:1504.06055 (2015)
4. Kalal, Z., Mikolajczyk, K., Matas, J.: Tracking-learning-detection. Pattern Analysis and Machine Intelligence, IEEE Transactions on **34**(7) (2012) 1409–1422
5. Bo, L., Ren, X., Fox, D.: Multipath sparse coding using hierarchical matching pursuit. In: Computer Vision and Pattern Recognition (CVPR), 2013 IEEE Conference on, IEEE (2013) 660–667
6. Krizhevsky, A., Sutskever, I., Hinton, G.E.: Imagenet classification with deep convolutional neural networks. In: Advances in neural information processing systems. (2012) 1097–1105

7. Girshick, R., Donahue, J., Darrell, T., Malik, J.: Rich feature hierarchies for accurate object detection and semantic segmentation. In: Computer Vision and Pattern Recognition (CVPR), 2014 IEEE Conference on, IEEE (2014) 580–587
8. Levi, G., Hassner, T.: Age and gender classification using convolutional neural networks. Computer Vision and Pattern Recognition Workshop (CVPRW), 2015 IEEE Conference on (2015)
9. Donahue, J., Hendricks, L.A., Guadarrama, S., Rohrbach, M., Venugopalan, S., Saenko, K., Darrell, T.: Long-term recurrent convolutional networks for visual recognition and description. arXiv preprint arXiv:1411.4389 (2014)
10. Li, H., Li, Y., Porikli, F.: Deeptack: Learning discriminative feature representations by convolutional neural networks for visual tracking. In: Proceedings of the British Machine Vision Conference. BMVA Press. (2014)
11. Li, H., Li, Y., Porikli, F.: Deeptack: Learning discriminative feature representations online for robust visual tracking. arXiv preprint arXiv:1503.00072 (2015)
12. Wang, L., Ouyang, W., Wang, X., Lu, H.: Visual tracking with fully convolutional networks. In: Proceedings of the IEEE International Conference on Computer Vision (ICCV). (2015) 3119–3127
13. Wang, N., Yeung, D.Y.: Learning a deep compact image representation for visual tracking. In: Advances in neural information processing systems. (2013) 809–817
14. Wang, N., Li, S., Gupta, A., Yeung, D.Y.: Transferring rich feature hierarchies for robust visual tracking. arXiv preprint arXiv:1501.04587 (2015)
15. Nam, H., Han, B.: Learning multi-domain convolutional neural networks for visual tracking. arXiv preprint arXiv:1510.07945 (2015)
16. Zhang, K., Liu, Q., Wu, Y., Yang, M.H.: Robust visual tracking via convolutional networks. arXiv preprint arXiv:1501.04505 (2015)
17. Danelljan, M., Hager, G., Shahbaz Khan, F., Felsberg, M.: Learning spatially regularized correlation filters for visual tracking. In: Proceedings of the IEEE International Conference on Computer Vision (ICCV). (2015) 4310–4318
18. Kuen, J., Lim, K.M., Lee, C.P.: Self-taught learning of a deep invariant representation for visual tracking via temporal slowness principle. Pattern Recognition **48**(10) (2015) 2964–2982
19. Hong, S., You, T., Kwak, S., Han, B.: Online tracking by learning discriminative saliency map with convolutional neural network. In: Proceedings of the 32nd International Conference on Machine Learning, 2015, Lille, France, 6–11 July 2015. (2015)
20. Kristan, M., Matas, J., Leonardis, A., Felsberg, M., Cehovin, L., Fernandez, G., Vojir, T., Hager, G., Nebehay, G., Pflugfelder, R.: The visual object tracking vot2015 challenge results. In: Proceedings of the IEEE International Conference on Computer Vision (ICCV) Workshops. (2015) 1–23
21. Geiger, A.: Probabilistic Models for 3D Urban Scene Understanding from Movable Platforms. PhD thesis, KIT (2013)
22. Andriluka, M., Roth, S., Schiele, B.: People-tracking-by-detection and people-detection-by-tracking. In: Computer Vision and Pattern Recognition, 2008. CVPR 2008. IEEE Conference on, IEEE (2008) 1–8
23. Fan, J., Xu, W., Wu, Y., Gong, Y.: Human tracking using convolutional neural networks. Neural Networks, IEEE Transactions on **21**(10) (2010) 1610–1623
24. Jin, J., Dundar, A., Bates, J., Farabet, C., Culurciello, E.: Tracking with deep neural networks. In: Information Sciences and Systems (CISS), 2013 47th Annual Conference on, IEEE (2013) 1–5



25. Bazzani, L., Larochelle, H., Murino, V., Ting, J.a., Freitas, N.D.: Learning attentional policies for tracking and recognition in video with deep networks. In: Proceedings of the 28th International Conference on Machine Learning (ICML-11). (2011) 937–944
26. Mnih, V., Heess, N., Graves, A., et al.: Recurrent models of visual attention. In: Advances in Neural Information Processing Systems. (2014) 2204–2212
27. Ba, J., Mnih, V., Kavukcuoglu, K.: Multiple object recognition with visual attention. arXiv preprint arXiv:1412.7755 (2014)
28. Jia, Y., Shelhamer, E., Donahue, J., Karayev, S., Long, J., Girshick, R., Guadarrama, S., Darrell, T.: Caffe: Convolutional architecture for fast feature embedding. arXiv preprint arXiv:1408.5093 (2014)
29. Russakovsky, O., Deng, J., Su, H., Krause, J., Satheesh, S., Ma, S., Huang, Z., Karpathy, A., Khosla, A., Bernstein, M., et al.: Imagenet large scale visual recognition challenge. International Journal of Computer Vision (2014) 1–42
30. Deng, J., Dong, W., Socher, R., Li, L.J., Li, K., Fei-Fei, L.: Imagenet: A large-scale hierarchical image database. In: Computer Vision and Pattern Recognition, 2009. CVPR 2009. IEEE Conference on, IEEE (2009) 248–255
31. Smeulders, A.W., Chu, D.M., Cucchiara, R., Calderara, S., Dehghan, A., Shah, M.: Visual tracking: an experimental survey. Pattern Analysis and Machine Intelligence, IEEE Transactions on **36**(7) (2014) 1442–1468
32. Kristan, M., Pflugfelder, R., Leonardis, A., Matas, J., Čehovin, L., Nebehay, G., Vojř, T., Fernandez, G., Lukežič, A., Dimitriev, A., et al.: The visual object tracking vot2014 challenge results. In: Computer Vision-ECCV 2014 Workshops, Springer (2014) 191–217
33. Cehovin, L., Kristan, M., Leonardis, A.: Is my new tracker really better than yours? In: Applications of Computer Vision (WACV), 2014 IEEE Winter Conference on, IEEE (2014) 540–547
34. Danelljan, M., Häger, G., Khan, F., Felsberg, M.: Accurate scale estimation for robust visual tracking. In: British Machine Vision Conference, Nottingham, September 1-5, 2014, BMVA Press (2014)

## A Offline training

Our tracker is able to improve its performance as it trains on more offline data. By observing more videos, GOTURN learns how the appearance of objects change as they move. We further analyze the effect of the amount of training data on our tracker’s performance in Figure 9. We see that the tracking errors drop dramatically as we increase the number of training videos. Our state-of-the-art results demonstrated in Section 6.1 were obtained after training on only 307 short videos, ranging from a few seconds to a few minutes in length, with an average of 52 annotations per video. Figure 9 indicates that large gains could be achieved if the training set size were increased by labeling more videos.

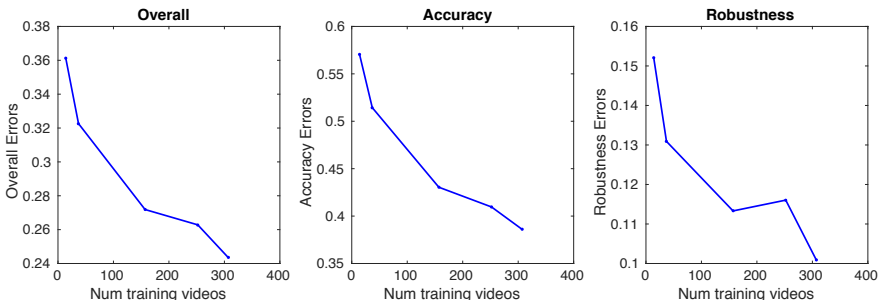


**Fig. 9.** Tracking performance as a function of the number of training videos (lower is better). This analysis indicates that large gains are possible by labeling more training videos.

## B Online training

Previous neural network trackers for tracking generic objects have been trained online [10,11,12,13,14,15,16,17,18,19]. Unfortunately, such trackers are very slow to train, ranging from 0.8 fps [10] to 15 fps [13], with the top performing neural-network trackers running at 1 fps [15,17,20]. In contrast, our tracker is trained offline in a generic manner, so no online training of our tracker is required. As a result, our tracker is able to track novel objects at 100 fps.

In Figures 10 and 11, we explore the benefits of online training. We use cross-validation to choose the online learning rate to be  $1e-9$ . Figure 10 shows that online training does not significantly improve performance beyond our offline training procedure. As might be expected, there is a small increase in robustness from online training; however, this comes at a cost of accuracy, since online training tends to overfit to the first few frames of a video and would not easily generalize to new deformations or viewpoint changes. A more detailed analysis is shown in Figure 11.

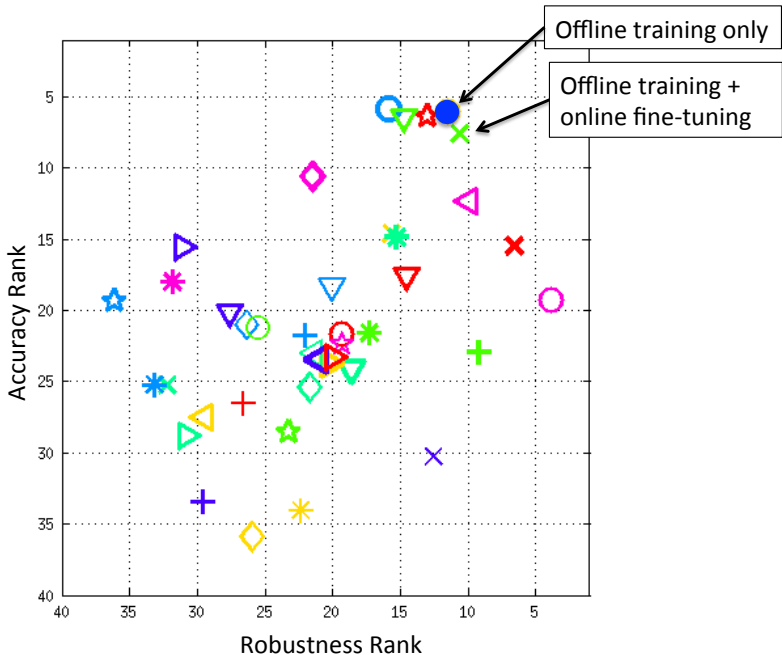


**Fig. 10.** Tracking results from the VOT 2014 tracking challenge. Our tracker’s performance is indicated with a blue circle, outperforming all previous methods on the overall rank (average of accuracy and robustness ranks). A version of our tracker with online training is shown with a green X. Both versions achieve approximately the same performance, demonstrating that our offline training procedure has already taught the network how to track a variety of objects.

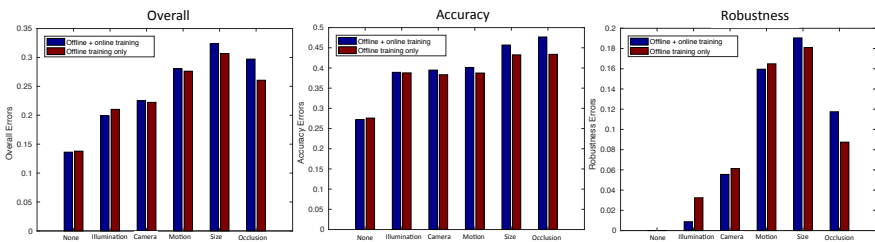


**Fig. 11.** Comparison of our tracker with and without online training (lower is better). Both versions achieve approximately the same performance, demonstrating that our offline training procedure has already taught the network how to track a variety of objects. Online training can lead to overfitting to the first few frames of a video, leading to more errors.

Our offline training procedure has seen many training videos with deformations, viewpoint changes, and other variations, and thus our tracker has already learned to handle such changes in a generic manner that generalizes to new objects. Although there might be other ways to combine online and offline training, our network has already learned generic target tracking from its offline training procedure and achieves state-of-the-art tracking performance without any online training required.

## C Generality vs Specificity

In Section 6.3, we analyze the generality of our tracker. We demonstrate that our tracker can generalize to novel objects not found in the training set. At the same time, a user can train our tracker to track a particular class of objects especially well by giving more training examples of that class of objects. This is useful if the tracker is intended to be used for a particular application where certain classes of objects are more prevalent.

We show more detailed results of this experiment in Figure 12. Analyzing the accuracy and robustness separately, we observe an interesting pattern. As the number of training videos increases, the accuracy errors decreases equally both for object classes that appear in our training set and classes that do not appear in our training set. On the other hand, the decrease in robustness errors is much more significant for object classes that appear in our training set compared to classes that do not.

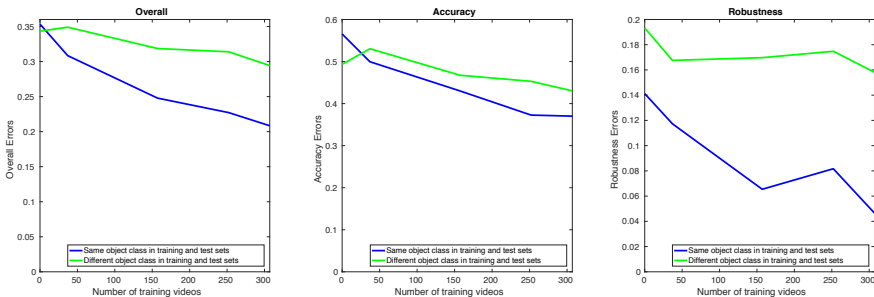


**Fig. 12.** Overall tracking errors for different types of objects in our test set as a function of the number of videos in our training set (lower is better). Class labels are not used by our tracker; these labels were obtained only for the purpose of this analysis.

Thus our tracker is able to learn generic properties about objects that enable it to accurately track new objects, i.e. to accurately denote the borders of the object with a bounding box. On the other hand, the tracker’s ability to generalize robustness is more limited; the tracker has a hard time tracking the motion of unknown objects when faced with difficult tracking situations. This analysis

points towards future work to increase the robustness of the tracker by labeling more videos or by learning to train on unlabeled videos.

## D Speed analysis

In Section 6.1, we showed the speed of our tracker as a function of the overall rank (computed as the average of accuracy and robustness ranks) and showed that we have the lowest overall rank while being one of the fastest trackers. In Figure 13 we show more detailed results, demonstrating our tracker’s speed as a function of the accuracy rank and the robustness ranks. Our tracker has the second-highest accuracy rank, one of the top robustness ranks, and the top overall rank, while running at 100 fps. Previous neural-network trackers range from 0.8 fps [10] to 15 fps [13], with the top performing neural-network trackers running at only 1 fps GPU [15,17,20], since online training of neural networks is slow. Thus, by performing all of our training offline, we are able to make our neural network tracker run in real-time.

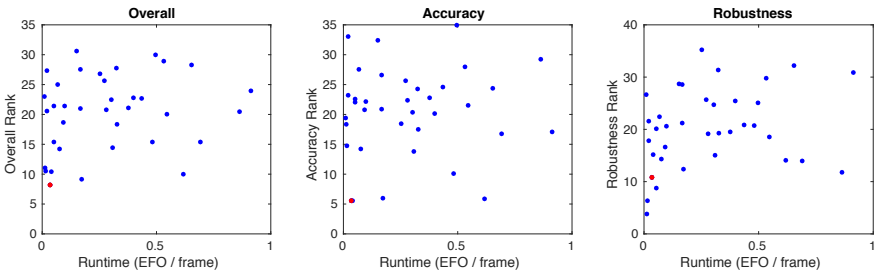


**Fig. 13.** Rank vs runtime of our tracker (red) compared to the 38 baseline methods from the VOT 2014 Tracking Challenge (blue). Each blue dot represents the performance of a separate baseline method (best viewed in color).

## E How does it work?

In Section 6.2, we explored how our tracker works as a combination of two hypotheses:

1. The network compares the previous frame to the current frame to find the target object in the current frame.
2. The network acts as a local generic “object detector” and simply locates the nearest “object.”

We distinguished between these hypotheses by comparing the performance of our network to the performance of a network which does not receive the previous

frame as input. In Figure 14 we show more details of this experiment, showing also accuracy and robustness rankings. For a more detailed interpretation of the results, see Section 6.2.

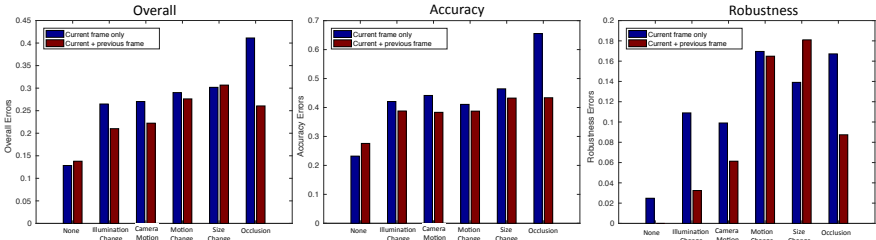


**Fig. 14.** Tracking errors for our network which receives as input both the current and previous frame, compared to a network which receives as input only the current frame (lower is better). This comparison allows us to disambiguate between two hypotheses that can explain how our neural-network tracker works (see Section 6.2).

## F Motion Smoothness Distribution

In Section 4.2, we describe how we use random cropping to implicitly encode the idea that small motions are more common than large motions. To determine which distribution to use to encode this idea, we analyze the distribution of object motion found in the training set. This motion distribution can be seen in Figure 15. As can be seen from this figure, each of these distributions can be modeled by Laplace distributions. Accordingly, we use Laplace distributions for our random cropping procedure. Note that the training set was only used to determine the shape of the distribution (i.e. Laplace); we use our validation set to determine the scale parameters for the distributions.

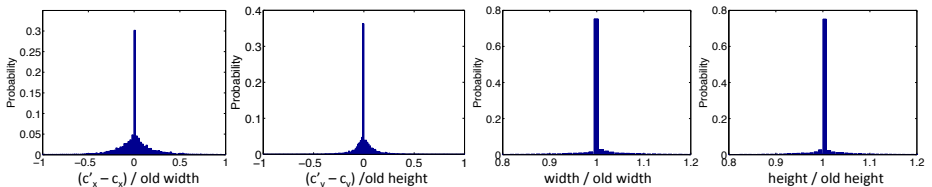


**Fig. 15.** Statistics for the change in bounding box size and location across two consecutive frames in our training set.

In more detail, suppose that the bounding box in frame  $t - 1$  is given by  $(c_x, c_y, w, h)$  where  $c_x$  and  $c_y$  are the coordinates of the center of the bounding box and  $w$  and  $h$  are the width and height accordingly. Then the bounding box at time  $t$  can be seen as drawn from a distribution:

$$c'_x = c_x + w \cdot \Delta x \quad (5)$$

$$c'_y = c_y + h \cdot \Delta y \quad (6)$$

$$w' = w \cdot \gamma_w \quad (7)$$

$$h' = h \cdot \gamma_h \quad (8)$$

with random variables  $\Delta x$ ,  $\Delta y$ ,  $\gamma_w$ , and  $\gamma_h$ , where  $(c'_x, c'_y, w', h')$  parameterize the bounding box at time  $t$  using the same representation described above. In terms of the random variables, we can rewrite these expressions as

$$\Delta x = (c'_x - c_x)/w \quad (9)$$

$$\Delta y = (c'_y - c_y)/h \quad (10)$$

$$\gamma_w = w'/w \quad (11)$$

$$\gamma_h = h'/h \quad (12)$$

The empirical distributions of these random variables over the training set are shown in Figure 15.

## G Training Set

Our training set was taken from ALOV300++ [31]. To ensure that there is no overlap with our test set, we removed 7 videos from our training set. These videos are:

- 01-Light\_video00016
- 01-Light\_video00022
- 01-Light\_video00023
- 02-SurfaceCover\_video00012
- 03-Specularity\_video00003
- 03-Specularity\_video00012
- 10-LowContrast\_video00013

After removing these 7 overlapping videos, there is no overlap between the videos in the training and test sets.

## H Detailed Results

The detailed results of our method compared to the 38 other methods that were submitted to the VOT 2014 Tracking Challenge [32] are shown in Table 2. The VOT 2014 Tracking Challenge consists of two types of experiments. In the

first experiment, the trackers are initialized with an exact ground-truth bounding box (“exact”). In the second experiment, the trackers are initialized with a noisy bounding box, which is shifted slightly off of the target object (“noisy”). For the noisy initialization experiment, the same 15 noisy initializations are used for each tracker, and the results shown are an average of the tracking performance across these initializations. This experiment allows us to determine the robustness of each tracker to errors in the initialization. This noisy initialization procedure imitates that of a noisy automatic initialization process or noisy human initializations.

The trackers are evaluated using two standard tracking metrics: accuracy and robustness [32,33]. Each frame of the video is annotated with a number of attributes: occlusion, illumination change, motion change, size change, and camera motion. The trackers are ranked in accuracy and robustness separately for each attribute, and the rankings are then averaged across attributes to get a final accuracy and robustness ranking for each tracker. The accuracy and robustness rankings are averaged to get an overall ranking, shown in Table 2.



Method name	Overall Ranks		Accuracy Ranks		Robustness Ranks		Speed Frames/EFO
	Exact	Noisy	Exact	Noisy	Exact	Noisy	
<b>GOTURN (Ours)</b>	<b>8.206944</b>	<b>8.588319</b>	5.544841	7.227564	10.869048	9.949074	29.928769
SAMF	9.970153	9.297234	5.866667	5.685897	14.073638	12.908571	1.617264
KCF	10.368056	9.341055	5.533730	5.583333	15.202381	13.098776	24.226259
DSST	9.193519	9.393977	5.979630	5.855556	12.407407	12.932399	5.803051
PLT <sub>14</sub>	10.526710	9.412576	14.720087	13.726667	6.333333	5.098485	62.846506
DGT	10.633462	9.880582	11.719306	9.318182	9.547619	10.442982	0.231538
PLT <sub>13</sub>	11.045249	11.066132	18.340498	17.298932	3.750000	4.833333	75.915548
eASMS	14.267836	12.838634	14.220760	11.327036	14.314912	14.350232	13.080900
HMMTxD	15.398256	14.663101	10.070087	9.727810	20.726425	19.598391	2.075963
MCT	15.376874	15.313581	16.806659	17.576278	13.947090	13.050884	1.447154
ABS	19.651999	15.340186	20.666961	15.344515	18.637037	15.335856	0.623772
ACAT	14.438846	16.338981	13.796118	17.769841	15.081575	14.908122	3.237589
MatFlow	15.393888	16.910356	21.996109	19.142094	8.791667	14.678618	19.083821
LGTv1	20.504135	18.189239	29.225131	26.533460	11.783138	9.845018	1.158273
ACT	18.676877	18.692439	20.756783	22.184568	16.596972	15.200311	10.858222
VTDMG	19.992574	18.835055	21.481942	20.647094	18.503205	17.023016	1.832097
qwsEDFT	18.365675	19.776101	17.495604	18.545589	19.235747	21.006612	3.065546
BDF	20.535189	19.905596	23.242965	21.731090	17.827413	18.080103	46.824844
Struck	21.038417	20.129413	20.868501	21.424688	21.208333	18.834137	5.953411
ThunderStruck	21.389674	20.333286	22.612468	21.989153	20.166880	18.677419	19.053603
DynMS	21.141005	20.479737	22.815739	21.510423	19.466270	19.449050	2.650560
aStruck	20.780963	21.465762	22.409722	20.878854	19.152203	22.052670	3.576635
SIR_PF	22.705212	22.413896	24.537547	22.331205	20.872878	22.496587	2.293901
Matrioska	21.371144	23.119954	22.115980	21.947863	20.626308	24.292044	10.198580
EDFT	22.516498	23.176905	20.338931	22.141689	24.694066	24.212121	3.297059
OGT	22.463076	23.528818	14.810633	16.893364	30.115520	30.164271	0.393198
CMT	22.788164	23.852773	20.098007	22.612765	25.478321	25.092781	2.507500
FoT	23.003472	24.375915	19.388889	21.623392	26.618056	27.128439	114.643138
IIVTv2	25.669987	24.610138	25.651061	25.400309	25.688913	23.819967	3.673112
IPRT	25.014620	25.081882	27.564283	26.643535	22.464957	23.520229	14.688296
PTp	27.288300	25.208133	33.046296	30.268937	21.530303	20.147328	49.892214
LT_FLO	23.958402	26.020573	17.075617	20.843334	30.841186	31.197811	1.096522
FSDT	28.275770	26.805519	24.378835	24.318730	32.172705	29.292308	1.529770
IVT	28.892955	27.820781	27.952576	27.432765	29.833333	28.208796	1.879526
IMPNCC	27.566645	29.293698	26.570580	29.349962	28.562711	29.237434	5.983489
CT	30.585835	29.377864	32.462103	30.823647	28.709566	27.932082	6.584306
FRT	27.800316	29.554293	24.300128	27.199856	31.300505	31.908730	3.093665
NCC	26.831924	30.305656	18.497180	23.444646	35.166667	37.166667	3.947948
MIL	30.007762	30.638921	34.934175	35.527778	25.081349	25.750064	2.012286

**Table 2.** Full results from the VOT 2014 tracking challenge, comparing our method (GOTURN) to the 38 other methods submitted to the competition. We initialize the trackers in two different ways: with the exact ground-truth bounding box (“Exact”) and with a noisy bounding box (“Noisy”).